Published in final edited form as:
Brain Res. 2007 February 9; 1132(1): 84–99. doi:10.1016/j.brainres.2006.11.055.

Opposing effects of spinal nerve ligation on calcium-activated potassium currents in axotomized and adjacent mammalian primary afferent neurons

Constantine D Sarantopoulos[1,2], **J Bruce McCallum**[1], **Marcel Rigaud**[1], **Andreas Fuchs**[1], **Wai-Meng Kwok**[1,2], and **Quinn H Hogan**[1]

1 *Department of Anesthesiology, Medical College of Wisconsin, 8701 Watertown Plank Road, Milwaukee, WI 53226*

2 *Department of Pharmacology & Toxicology, Medical College of Wisconsin, 8701 Watertown Plank Road, Milwaukee, WI 53226*

Abstract

Calcium-activated potassium channels regulate AHP and excitability in neurons. Since we have previously shown that axotomy decreases I_{Ca} in DRG neurons, we investigated the association between I_{Ca} and $K_{(Ca)}$ currents in control medium-sized (30–39 μM) neurons, as well as axotomized L5 or adjacent L4 DRG neurons from hyperalgesic rats following L5 SNL. Currents in response to AP waveform voltage commands were recorded first in Tyrode's solution and sequentially after: 1) blocking Na^+ current with NMDG and TTX; 2) addition of $K_{(Ca)}$ blockers with a combination of apamin 1μM, iberiotoxin 200 nM, and clotrimazole 500 nM; 3) blocking remaining K^+ current with the addition of 4-AP, TEA-Cl, and glibenclamide; and 4) blocking I_{Ca} with cadmium. In separate experiments, currents were evoked (HP −60 mV, 200 ms square command pulses from −100 to +50 mV) while ensuring high levels of activation of $I_{K(Ca)}$ by clamping cytosolic Ca^{2+} concentration with pipette solution in which Ca^{2+} was buffered to1μM. This revealed $I_{K(Ca)}$ with components sensitive to apamin, clotrimazole and iberiotoxin. SNL decreases total $I_{K(Ca)}$ in axotomized (L5) neurons, but increases total $I_{K(Ca)}$ in adjacent (L4) DRG neurons. All $I_{K(Ca)}$ subtypes are decreased by axotomy, but iberiotoxin-sensitive and clotrimazole-sensitive current densities are increased in adjacent L4 neurons after SNL. In an additional set of experiments we found that small sized control DRG neurons also expressed iberiotoxin–sensitive currents, which are reduced in both axotomized (L5) and adjacent (L4) neurons.

Conclusions: Axotomy decreases $I_{K(Ca)}$ due to a direct effect on $K_{(Ca)}$ channels. Axotomy-induced loss of I_{Ca} may further potentiate current reduction. This reduction in $I_{K(Ca)}$ may contribute to elevated excitability after axotomy. Adjacent neurons (L4 after SNL) exhibit increased $I_{K(Ca)}$ current.

Author for correspondence: Constantine D. Sarantopoulos, MD, PhD, Department of Anesthesiology, Medical College of Wisconsin, MEB, 8701 Watertown Plank Road, Milwaukee, WI 53226, Phone: (414) 456 5733/Fax: (414) 456 6507/e-mail: E-mail: csar@mcw.edu.

Part of the study has been presented as a poster at the 35th Society for Neuroscience Meeting, Washington, DC, 2005.

The study was supported by NIH NS42150 (QHH) and NINDS S049420A (CDS)

Keywords

dorsal root ganglion; nerve injury; neuropathic pain; calcium-activated potassium channels; apamin; iberiotoxin; clotrimazole

Introduction

Neuropathic pain frequently accompanies common diseases, such as diabetes, herpes zoster, herniated nucleus pulposus, or direct nerve trauma [96,97], manifests with unpleasant spontaneous sensations, allodynia, and hyperalgesia [73], and is resistant to most conventional treatments [48,85]. In addition, diseases such as diabetes are also accompanied by hypoalgesia and sensory deprivations. Pertinent animal models have identified important pathogenic processes contributing to increased excitability at the site of injury as well as in the somata of sensory neurons proximal to the site of nerve trauma [45,91,103]. In this context, we have previously shown that experimental injury leading to behavioral manifestations of neuropathic pain is associated with diminished calcium influx through high-voltage-activated [34] and low-voltage-activated calcium channels [60].

Calcium influx via voltage-gated calcium channels (VGCC) regulates a diversity of cellular functions [5], including membrane excitability via modulation of $K_{(Ca)}$ channels. However, little is known about the role and contribution of these channels in the pathogenesis of neuropathic pain, although they may link reduced I_{Ca} with neuronal hyper-excitability and other phenomena observed in neuropathic states. It is well known that $K_{(Ca)}$ channels regulate several functions pertinent to normal sensory as well as to neuropathic pain transduction, such as modulating AHP, controlling the repolarization and duration of the AP, suppressing membrane excitability, setting inter-spike interval, mediating spike-frequency adaptation and controlling neurotransmitter release [90]. Three major families of $K_{(Ca)}$ channels have been identified in neurons, each with distinct structure, and pharmacological and biophysical properties, including single-channel conductance in symmetrical K^+ solutions. Large-conductance BK channels are voltage-gated and sensitive to iberiotoxin, whereas small-conductance SK channels are sensitive to apamin, and intermediate-conductance IK channels are sensitive to clotrimazole [22,77,78,90]. While BK channels require membrane depolarization for their activation, both SK and IK are voltage insensitive [17].

The coordinated activation of different $K_{(Ca)}$ current components regulates the AP time course and repetitive firing properties of neurons. BK channels participate in AP repolarization and conduct the current (traditionally named "I_C") underlying the fast AHP [17,78], whereas SK channels do not affect AP repolarization, but convey the $I_{(AHP)}$ that mediates the medium and slow AHP. The presence and role of $I_{K(Ca)}$ channels in neurons is unclear [78]. Altered regulation of AP kinetics and repetitive firing is particularly important in the pathogenesis of increased excitability of peripheral sensory neurons after nerve injury [80]. Nevertheless, the presence of different categories of $K_{(Ca)}$ channels in primary afferent neurons, as well as the influence of injury on these channels, is incompletely investigated [4]. Some studies have implied the presence of all three subtypes in DRG neurons, based on Ca^{2+}-dependence, sensitivity to $K_{(Ca)}$ blockers, and to electrophysiological features [3,4,57,83]. A previous study indicated that axotomy decreased $K_{(Ca)}$ channel conductance through loss of I_{Ca} alone, with no effect on the $K_{(Ca)}$ channel directly [1].

On the basis of these prior observations, we hypothesized that $I_{K(Ca)}$ is normally present in medium sized DRG somata. As the presence and roles of specific $K_{(Ca)}$ channel subtypes in primary afferent neurons is unresolved, we investigated the expression of SK, IK or BK in acutely dissociated DRG neurons. Elevated neuronal excitability constitutes a cardinal feature

of neuropathy, so the fact that $K_{(Ca)}$ currents modulate parameters that determine neuronal excitability implicates a role for altered $K_{(Ca)}$ function. As peripheral nerve injury results in altered performance and expression of I_{Ca}, I_K, and I_{Na}, it is highly likely that injury may likewise affect $K_{(Ca)}$ channels directly. Thus, the goal of this investigation has been to investigate the presence of $I_{K(Ca)}$ in mammalian primary afferent neuronal somata, and to identify the effect of nerve injury after SNL, a standard model of experimental neuropathic pain [47].

Dorsal root ganglion neuronal somata are classified based on morphological (size) and electrophysiological characteristics (AP parameters, conduction velocity) into small, medium and large. These correspond to somata of C, Aδ and Aβ nerve fibers, respectively, that mediate different physiological functions. Medium sized somata correspond to Aδ fibers, that contain a heterogeneous population of neurons containing nociceptors and non-nociceptors (low threshold mechanoreceptors) [50]. We therefore chose to focus on this representative population. Several studies have indicated that medium sized somata with axons of Aδ-fiber caliber exhibit significant phenotypic changes after nerve injury, and may be an important generator of ectopic discharges [11,23,53,55,56,63,98]. In addition, a previous study from our lab showed that Aδ fibers exhibited the most pronounced electrophysiological changes after SNL, and in particular increased AP duration, decreased AHP amplitude and duration, and increased repetitive firing during sustained depolarization, manifestations that may explain increased neuronal excitability and hyperalgesia in neuropathic pain states [80].

In addition to the axotomized neurons, adjacent neurons may contribute to pathogenesis of the neuropathic phenotype [20,23,40,58,98]. We therefore additionally investigated $I_{K(Ca)}$ in medium sized neuronal somata dissociated from the L4 DRG that share the sciatic nerve with degenerating distal segments of the axotomized L5 neurons after SNL.

Finally, we also examined small sized neuronal somata (diameter<30 μm) obtained from control, axotomized (L5) and adjacent (L4) DRGs for the presence of iberiotoxin sensitive (BK) current. Small DRG neurons correspond mostly to Aδ and C type nociceptors, and there is strong evidence about the presence of BK channels in this population, wherein they reduce the amount of Ca^{2+} influx during an AP, as well as they limit repetitive firing activity in these cells [83].

Results

Medium sized cells were obtained from rats with SNL (n=28) exhibiting 39.5±17.9% hyperalgesic response rates, and from and sham-operated rats (n=25) with 0±0% hyperalgesic response rates (Mann Whitney U = 0, p<0.001). Small cells were dissociated from rats with SNL (n=10) exhibiting 39.1±23.5% hyperalgesic response rates and sham-operated rats (n=4) with 0±0% hyperalgesic response rates (Mann Whitney U = 0, p=0.002). Hyperalgesic responses were sustained paw lifting, shaking and licking in response to nociceptive mechanical stimulation (application of the tip of a 22 gauge spinal needle) [33].

We studied 144 medium-sized neuronal somata with diameter 34.32±2.05 μm and capacitance 50.32±19.51 pF (mean±SD). In addition, we studied 27 small-sized neurons with diameter 25.06±2.12 μm and capacitance 37.59±8.91 pF (mean±SD). These values are in agreement with data previously published in the literature regarding medium and small sized DRG neuronal somata by us [34,82] and other investigators [76].

Primary afferent neurons express $I_{K(Ca)}$

Since axotomy decreases I_{Ca} in DRG neurons [1,34,60], we first investigated the possible association between I_{Ca} and $I_{K(Ca)}$ in control neurons (n=13). Currents were recorded by

conventional whole-cell patch-clamp technique [28]. In order to examine cells under conditions more closely simulating the natural electrical activity of each neuron *in vivo*, currents were elicited by voltage commands in the form of an AP waveform, recorded from each neuron in Tyrode's solution (Figure 1). Baseline whole-cell currents were elicited in Tyrode's solution, and then sequentially after blocking: 1) I_{Na} by substituting NaCl in Tyrode's with equimolar NMDG, and with 0.3 μM TTX; 2) $I_{K(Ca)}$ with apamin (1 μM), iberiotoxin (200 nM), and clotrimazole (500 nM) in combination; 3) remaining K^+ current with the addition of 4-AP (1 mM), TEA-Cl (160 mM), and glibenclamide (1 μM); and 4) I_{Ca} with cadmium 200 μM (Figure 1). This allowed derivation of the difference current attributable to I_{Ca}, $I_{K(Ca)}$, and total I_K ($I_{K(tot)}$). I_{Ca} measurements were made in the same cells from which $I_{K(Ca)}$ measurements and $I_{K(tot)}$ measurements were made.

With regard to these $I_{K(Ca)}$ blockers, apamin is a selective blocker of SK channels with IC_{50} 63 pM for the SK2, 2 nM for the SK3 subtype, and a range between 3.3 and 12 nM for SK1 [78]. Iberiotoxin selectively blocks BK channels with IC_{50} in the low nM range [54], and clotrimazole blocks IK channels with IC_{50} 50 nM [22].

Control neurons exhibited significant $I_{K(Ca)}$, determined as current sensitive to apamin, iberiotoxin and clotrimazole combined (Figure 2).

Total $I_{K(Ca)}$ is increased in axotomized neurons but decreased in adjacent neurons

Similar recordings were obtained from axotomized L5 neurons (n=14) and adjacent to injuy L4 neurons (n=13) from rats subjected to SNL (Figure 3). Resting membrane potential did not differ amongst the three groups (−60.54±2.83mV in control, −56.18±1.84 mV in SNL L5, and −56.42±1.90 in SNL L4; p=0.311 by one way ANOVA). Membrane capacitance was 51.92 ±18.47 pF in control, 64.82±17.15 pF in L5 SNL and 48.46±20.32 pF in L4 neurons. Mean diameter was 35.42±1.77 μm for control, 34.77±1.63 μm for L5 SNL, and 34.37±1.79 μm for L4 neurons. Neither membrane capacitance, nor diameter differed among the three cell populations (p n.s. for membrane capacitance and cell diameter, respectively).

Individual current densities were determined in experiments wherein each cell was depolarized sequentially using its own AP waveform as a voltage command. Each current component (including I_{Na}) was determined as a difference current, after subtracting the trace recorded during blockade of this particular current component from the immediately preceding current trace (except $I_{K(tot)}$ which was estimated by subtracting the current after all I_K blockers from that in NMDG-Tyrode's). Thus peak I_{Na} was determined by subtracting the current trace during NMDG and TTX, from the trace recorded in regular Tyrode's solution. Because NMDG substitution for Na^+ ions blocks I_{Na} generally, and TTX blocks TTX-sensitive sodium channels, subtraction is expected to reveal the difference trace, representing the inward I_{Na}. In a similar methodology, $I_{K(Ca)}$ was determined by subtracting the current after administration of $K_{(Ca)}$ blockers from that in NMDG-Tyrode's, and so forth. Peak currents were measured from these difference traces, while charge transfer values from the corresponding AUC. Traces were normalized for capacitance to obtain current densities.

Peak I_{Na} density (p n.s.) and charge transfer (p n.s.) did not differ among the three cell types.

However, peak $I_{K(Ca)}$ density differed amongst the three cell types (p=0.005, by analysis of variance). Post hoc tests showed that peak $I_{K(Ca)}$ density was less in axotomized (L5 SNL) somata compared to adjacent L4 somata (p=0.001), while the latter exhibited significantly higher peak current density compared to control somata (p=0.031). All other post-hoc comparisons did not reveal any significant differences. Charge transfer sensitive to $K_{(Ca)}$

inhibitors also differed amongst the three cell types (p=0.029). Post hoc comparisons showed that $K_{(Ca)}$ charge transfer was also less in axotomized (L5 SNL) somata compared to adjacent (L4) somata (p=0.01), while a marginal difference was shown between control and L4 SNL (p=0.057).

Peak current density for total I_K, determined as current sensitive to all potassium channel blockers (4-AP, TEA-Cl, and glibenclamide in addition to apamin, iberiotoxin and clotrimazole) also differed amongst the different neuronal populations (p=0.001). The same was the case for total potassium charge transfer (p=0.02). Post hoc comparisons showed that peak current density for total I_K sensitive to all potassium channel blockers (4-AP, TEA-Cl, and glibenclamide in addition to apamin, iberiotoxin and clotrimazole) was less in axotomized SNL L5 neurons compared to adjacent L4 somata (p<0.001), and was increased in SNL L4 compared to control (p=0.005). The same pattern was evident in charge transfer of total potassium current (SNL L4 vs. L5, p=0.009; SNL L4 vs. control, p=0.025).

Mean peak $I_{K(Ca)}$ in L5 SNL was decreased compared to control by 72.58 pA/pF, while in L4 increased compared to control by 142.95 pA/pF. Mean peak of total I_K in L5 SNL decreased by 65.98 pA/pF (close to the calculated reduction of the $I_{K(Ca)}$ component). In L4, total I_K increased by 214.76 pA/pF from control, which is more than the amount of increase in $I_{K(Ca)}$ from control. These differences indicate that the reduction in the overall I_K is mainly due to loss of $I_{K(Ca)}$, while elevation in other I_K subtypes other than $I_{K(Ca)}$ may account for the increased total I_K in L4.

Finally, peak I_{Ca} density (p n.s.) and Ca^{2+} charge transfer (p n.s.) did not differ significantly amongst the different neuronal populations.

$I_{K(Ca)}$ in DRG neuronal somata has components selectively sensitive to apamin, clotrimazole and iberiotoxin (Figure 4)

In a second series of experiments, K^+ currents were recorded during square wave voltage commands (HP −60mV, 200ms pulses from −100 to +50mV; Figure 4). In order to ensure high levels of opening of $K_{(Ca)}$ channels, and thereby identify channel function independent of variability of I_{Ca} between neurons, the cytosol was dialyzed with pipette solution in which the calculated final free $[Ca^{2+}]_i$ was clamped at 1 μM in all three cell types. By clamping the intracellular $[Ca^{2+}]$ to 1 μM, differences in $I_{K(Ca)}$ between the control, axotomized L5 and adjacent L4 neurons is attributable to an injury effect on the $K_{(Ca)}$ channel directly, eliminating any contribution due to altered I_{Ca}.

Separate administration of each of the $K_{(Ca)}$ channel blockers apamin (1 μM), iberiotoxin (200 nM) and clotrimazole (500 nM) resulted in significant current reduction from baseline in medium-sized control neuronal somata dissociated from SS rats (p=0.01, n=22 for the main effect of apamin; p<0.001, n=16 for the iberiotoxin effect; and p=0.051, n=12, for the clotrimazole effect; Figure 4).

Injury effects on $I_{K(Ca)}$ in axotomized and adjacent neurons are subtype-selective (Figure 5)

In contrast to control neurons (n=22), in which apamin reduced potassium current, SNL L5 neurons (n=12) and SNL L4 neurons (n=9) showed no significant current reduction with this agent. Comparatively, L5 neurons had significantly less apamin-sensitive current than control neurons (p=0.025) (Figure 5A).

The average apamin sensitive current is inward at negative membrane potentials in L5 SNL medium sized cells (Figure 5A). Half of these cells exhibited an inward current component at membrane potentials more negative than −60 mV at baseline. Apamin in these cells blocked the current both at positive as well as at negative membrane potential, but the latter to a degree that a small negative component (less than -10 pA/pF) still remained. Of note is the fact that other investigators have reported an inward component in apamin-sensitive currents in the range of negative membrane potentials [31].

Considering responses to apamin in axotomized SNL L5 neurons, analysis of our findings revealed two distinct groups of neurons. The first group (n=6 out of 12) responded to administration of apamin with a very large reduction of current. In the second group of neurons (n=5 out of 12), apamin produced either no change of the current or a minimal response. In one cell, administration of apamin produced a pronounced increase of current above the baseline, thus the difference current was negative. This was not the case in control neurons, wherein apamin blocked the baseline current in the majority of cells (n=17 out of 22). We obtained the result shown in Figure 5A by averaging the difference currents from each individual cell, thus the large error bars represent this significant variability.

Iberiotoxin reduced potassium current in SNL L5 neurons (n=9, p=0.031) and SNL L4 neurons (n=8, p=0.001) as well as control neurons. The effect action of iberiotoxin was significantly less in SNL L5 neurons compared to control (p<0.001), but significantly greater in SNL L4 neurons compared to control (p=0.001) (Figure 5B). Clotrimazole produced significant current blockade in SNL L4 neurons (p<0.001, n=7) in addition to control, but injury precludes an effect of clotrimazole in SNL L5 neurons (p=0.1, n= 9). As in the case of iberiotoxin, clotrimazole-sensitive current density was decreased in axotomized SNL L5 somata compared to control (p=0.022), but increased in adjacent L4 neurons (p<0.001)(Figure 5C).

The degree by which each blocker (apamin, iberiotoxin and clotrimazole) inhibited current in each cell type, expressed as percent inhibition from baseline at +40 mV membrane potential, is shown in Figure 6.

Small sized neurons express iberiotoxin-sensitive current, reduced by SNL (Figure 5D)

Separate experiments on small sized control neurons (n=6) using square wave voltage commands (HP −60mV, 200ms pulses from −100 to +50mV) and clamping intracellular [Ca^{2+}] to 1 μM, revealed iberiotoxin sensitive currents. There was a significant main effect of injury with regard to the amplitude of this current (p<0.001), while post hoc comparisons showed that amplitude is diminished by SNL in both axotomized L5 (n=9, p<0.001) and adjacent L4 neuronal somata (n=12, p<0.001) compared to control (Figure 5D).

Discussion

In this study, we have demonstrated the presence of current sensitive to standard $K_{(Ca)}$ channel blockers in medium-sized somata dissociated from rat DRG, confirming the findings of others [2–4,7,24,57,83]. This current contains components sensitive to apamin, iberiotoxin and clotrimazole, which are consistent with potassium currents via SK, BK and IK channels. A critical novel finding of our study is that axotomy decreases this $I_{K(Ca)}$, while medium sized somata at the neighboring L4 DRG respond with increased current. Further, the injury effect is not uniform across all current subtypes.

Our techniques allow us to conclude that the $I_{K(Ca)}$ changes we observed are independent of underlying variability of I_{Ca} and subsequent $K_{(Ca)}$ channel activation. This is true in the first

set of experiments because concurrently measured I_{Ca} did not differ between the groups, although $I_{K(Ca)}$ was less in SNL L5 neurons and higher in SNL L4 neurons. In the second set, I_{Ca} was blocked with cadmium while intracellular Ca^{2+} concentration was clamped at 1μM, which is sufficient to ensure near maximal activation of $K_{(Ca)}$ channels [29], and thereby eliminate any variability due to I_{Ca}. Thus, our findings indicate a direct effect of axotomy on $K_{(Ca)}$ channels independent of alterations in I_{Ca}. This contrasts with a previous report in which the axotomy-induced effect was driven by decreased I_{Ca} alone [1]. However, these investigators used a distal sciatic nerve transection, which fails to provide a distinct axotomized and adjacent neuronal population, so divergent effects may have been negated in their findings.

A possible shortcoming in our protocols is a main focus on a single size group of neuronal somata. We selected medium-sized neurons since they include nociceptors, and because they constitute a physiologically relevant cellular population that develops increased excitability after nerve injury [58,80]. Several studies have indicated that this neuronal population exhibits the most significant phenotypic changes after nerve injury [11,23,53,55,56,63,80,98]. Our observations on iberiotoxin-sensitive current in small neurons demonstrates that injury-related effects on primary afferent neurons are not unique to the medium size group.

Our study was not designed to assess alterations of neuronal soma size (measured either by diameter or capacitance) after axotomy. In order to stratify cells by size (as medium- or small-sized), we selected neuronal somata within the same apparent diameter range in each experimental group, and we ended up obtaining similarly sized control, axotomized and adjacent neurons. Thus we studied neurons of the same apparent diameter among different groups, but capacitance values also did not differ amongst control, axotomized and adjacent to injury neurons (although axotomized L5 somata exhibited a non-statistically-significant capacitance increase versus control and adjacent L4 cells). An enlargement of neuronal soma size often ensues following axotomy. Moore and Thanos demonstrated that two weeks after optic nerve axotomy or crush, mean ganglion soma size increased in either type of injury. However, while soma size at four weeks remained increased (60% larger than normal) only after crush injury, this was not the case after axotomy, wherein mean cell size had returned to normal levels by that time [64]. Considering the time course of our experimentation (approximately 3 weeks from the time of axotomy by SNL), it is likely that we might have also missed any axotomy-induced soma enlargement that might have occurred at a much earlier time after SNL, and then regressed. Other investigators have shown that the mean soma size of axotomized sacral peripheral parasympathetic ganglion neurons was significantly smaller than that of uninjured neurons [92], but neither this was the case in our study.

The concentrations of EGTA we used in the internal pipette solution (2–5 mM) may be considered as relatively high for neuronal cells. Nevertheless, for the duration of our recordings we did not observe any aberrant morphological or electrophysiological alterations indicative of unusual cellular phenomena, and we were able to record pertinent electrophysiological activity in the usual fashion. We have also used similar concentrations in neurons in previously published studies without problems [34,81], including studies of potassium currents [82]. Other investigators have similarly used EGTA concentrations in this range (3 mM EGTA) for studying $I_{K(Ca)}$ currents in neurons [83]. However, EGTA concentrations, such as the ones we used in our study, may affect Ca^{2+}-dependent physiological processes at primary afferent somata, and this may constitute a limitation. Huang and Neher have shown that 5 mM EGTA may affect exocytosis evoked by short depolarizations in DRG neurons [39]. Furthermore, Gabso et al have shown that high concentrations of buffers may have profound effects on processes that depend on the concentration and kinetics of intracellular Ca^{2+} [21]. Thus, we cannot exclude the possibility that the EGTA concentration we used might have affected the activation of $K_{(Ca)}$ channels, although this has been not shown directly in the previous two reports, which were only pertinent to effects on other processes. In any case, we do not think

that high EGTA concentrations might have confounded our results since all of our cells (control as well as axotomized and adjacent) were exposed to the same experimental conditions, and thus to the same intracellular concentrations of EGTA. So differences observed among these cell types cannot be attributed to this factor. Recordings at room temperature may also not simulate natural conditions for a neuron. Nevertheless, all recordings from all neurons were obtained at the same temperature, thus this may not be a confounding factor regarding the observed differences.

Another limitation of our study is the inability to know specifically, in the absence of specific dye labeling, whether the L4 neurons under study project to the sciatic nerve. The majority of all sciatic nerve primary afferent neuronal somata in the rat are located in the L4 and L5 DRGs [88]. Yip et al reported that localized horseradish peroxidase injection into crushed sciatic nerve of rats labels most neurons in L4 and L5 DRG [101]. Although in the rat the L4 DRG neuronal population is the major contributor of axons into the sciatic nerve, containing approximately 60% of the total sciatic DRG neurons [88], not all L4 DRG neurons project into the sciatic nerve [52]. Few L4 DRG neurons also dichotomize into two or more axons, each one projecting into different nerves [88]. Devor et al, using electrophysiological and retrograde trace transport methods, showed that approximately 46–52% of the adult rat L4 DRG myelinated nerve fibers project into the sciatic nerve [13]. Additionally, Lewis et al, counting c-jun-expression neuronal profiles after sciatic nerve section in adult rats, estimated that approximately 55–60% of L4 DRG neurons project into the sciatic nerve [52]. Thus, since these L4 neurons remain intact in the SNL model we used, the L4 DRG after SNL contains neurons that share a distal nerve with degenerating L5 segments, and others (approximately 40–50%) that are unaffected. This may result in a potential dilution of our findings in L4 neurons after SNL, so our findings underestimate the real magnitude of the effect of nerve injury on these neurons.

We have used mainly pharmacological criteria to identify that the ionic currents we measured are carried by K^+ ions through $K_{(Ca)}$ channels. Specifically, pharmacological selectivity of apamin, iberiotoxin and clotrimazole reliably identifies these currents as carried by SK, BK and IK channels [77].

Voltage commands in the form of APs, as used in our study, are a more physiologically relevant way to elicit currents than sustained square waves, since they incorporate the kinetic aspect that the cell's membrane normally encounters, and they produce currents that represent the ionic fluxes during the natural AP [12,62]. All currents, including $I_{K(Ca)}$, were investigated with the same voltage protocol in these experiments. Our technique of sequential application of selective blockers further enabled us to separate various current components by subtraction.

Similar to other studies [31,87,99], the square voltage protocols we used in the second set of experiments had a duration of 200 ms, which may be considered inadequate for SK activation. However, SK channels are voltage insensitive [17,77,78], and in neurons these channels are typically activated by Ca^{2+} influx during actions potentials, which are of much shorter duration. Finally, the 200 ms pulses we employed were the same for all cells under investigation, so they are unlikely to have confounded our findings.

We have confirmed previous reports that primary afferent neurons express SK and IK channels, wherein they attenuate nociceptive afferent excitability [4,7,30]. Although others have raised uncertainty about the presence of IK channels in DRG neurons [42,44,77,78], our identification of a clotrimazole-sensitive current suggests that a component of $I_{K(Ca)}$ in these neurons is IK. Other prior observations also support our finding of BK currents in DRG somata [83,102]. Current through these channels contributes to the early AHP, prolongs the refractory period, and limits repetitive firing. Additionally, BK current shortens AP duration by accelerating repolarization, thereby limiting the amount of Ca^{2+} influx during an AP and thereby decreasing

neurotransmitter release [38,72,75]. Our methods characterizing $I_{K(Ca)}$ in sensory neurons adds validity to these previous findings by using methods that employ a natural AP waveform stimulus in one case, and by controlling cytoplasmic Ca^{2+} levels in the other.

Our results regarding apamin-sensitive currents indicate the presence of two distinct cellular groups in axotomized (L5) DRG medium sized somata, a cellular population non-responsive to apamin indicating loss of SK channels after SNL, and another subgroup wherein axotomy after SNL does not affect sensitivity to apamin. This variability may be attributed to either the presence of non–injured neurons in the L5 DRG, which contain axons projecting to the non-axotomized dorsal primary rami, or heterogeneity between cells with regards to responses after axotomy. The presence and redistribution after SNL of channels of SK1 subtype, which may not be very sensitive to apamin, may be another explanation, (but see [4]).

We did not directly investigate changes of AP and AHP in this study. Standard patch amplifiers are limited by voltage distortion in current-clamp mode, and may not obtain accurate recordings of excitability parameters [59]. However, using intracellular microelectrode recordings from intact, excised DRGs, we have previously noted that axotomy substantially increases AP duration and decreases the amplitude, duration and area of AHP in Aδ neurons, compared with other groups [80]. BK currents determine AP repolarization and AP duration, as well as fast AHP, while SK currents are responsible for the medium AHP [78]. So, in this context, our current findings in L5 medium sized neurons are compatible with our findings in intact ganglia. In the latter study, however, no important changes were evident in the L4 neurons, in contrast to our present results. It is possible that increased $I_{K(Ca)}$ in L4 neurons might compensate for other injury effects and keep the AP and AHP within the normal range. Another explanation may be pertinent to different methodologies used in the two studies. Cytoplasmic dialysis during whole-cell recordings and neuronal dissociation may introduce cellular aberrations compared to the less intrusive microelectrode recording from intact ganglia in our earlier study.

Axotomized primary afferent somata develop hyper-excitability that may contribute to the generation of neuropathic pain [14,15,45]. Considering the physiological functions of $I_{K(Ca)}$, it is possible that the injury-associated current loss we have noted after axotomy contributes to sensory neuron hyperactivity subsequently leading to neuropathic pain [3,37,100]. Our findings indicate that $K_{(Ca)}$ currents decrease in axotomized medium-sized DRG neurons, wherein coincide with increased excitability (such as increased AP duration, decreased AHP and repetitive firing during depolarization). Specifically, the decreased AHP we have previously noted [80] may be directly attributed to diminished $I_{K(Ca)}$, and the increased repetitive firing in axotomized L5 neurons, but not in adjacent L4 neurons after SNL, may be consistent with the divergent effect of SNL on $I_{K(Ca)}$ noted in the present study.

Although the relative contribution of alterations in injured versus uninjured afferents in the pathogenesis of neuropathic pain after SNL remains unclear [23,74], increased excitability in axotomized neurons, subsequent to $I_{K(Ca)}$ loss, may be pertinent to generation of behavioral manifestations of neuropathic pain, i.e. spontaneous pain and hyperalgesia. Aberrant firing of injured peripheral nerves definitely contributes to the manifestations of neuropathic pain [25, 68], while excitability changes secondary to alterations of $K_{(Ca)}$ currents have already been implicated in the pathogenesis of this ectopic spontaneous firing on injured primary afferent neurons [3,100]. Inhibition of $K_{(Ca)}$ channels by norepinephrine has been also implicated in the membrane hyper-excitability and hyperalgesia after chronic constriction sciatic nerve injury [37]. Spontaneous firing develops also in injured myelinated afferents after SNL [53], thus our findings that axotomized myelinated -but not adjacent uninjured afferents- develop increased excitability, and axotomized medium-sized fibers lose $I_{K(Ca)}$, contribute additional support to the argument that injured (and not uninjured) myelinated afferents mediate neuropathic pain behavior after SNL [6]. Because BK channels control neurotransmitter release

[86] and inter-neuronal glutaminergic synaptic efficacy [72], it is also likely that loss of BK currents in small and medium sized neurons after axotomy may enhance synaptic transmission of afferent signaling, as well. In addition to loss of $I_{K(Ca)}$ currents in a manner directly related to nerve injury, we have also previously shown that neuropathy decreases I_{Ca} [60,61], a mechanism that may reduce the activation of $K_{(Ca)}$ currents in addition to the direct effect of SNL, thus leading to a higher enhancement of excitability.

Although axotomized neurons (L5 ganglion after SNL) are disconnected from sensory fields, they are highly relevant to the generation of neuropathic pain. Neuronal excitation follows not only natural receptive field stimulation, but also other important forms of activation of the DRG somata after injury, including direct mechanical stimulation, depolarization by circulating and local algogens and inflammatory mediators, and sympathetic activity [14,69, 70,91]. Furthermore, cross-excitation spreads activity among adjacent neurons in the DRG [15]. This is highly relevant, since the L5 dorsal primary ramus of the spinal nerve remains intact after SNL, and most clinical nerve injuries are partial.

Our findings of increased current sensitive to $K_{(Ca)}$ blockers in L4 neurons adjacent to axotomized neurons is consistent with the decreased excitability (elevated perception thresholds) of surviving sensory pathways in humans [9,51].

We also provide further confirmation of the presence of BK current in small DRG cells [83]. Decreased iberiotoxin-sensitive current in small cells may also be pertinent in explaining changes after nerve injury. Considering that BK currents modulate the fast AHP of neurons, our findings may partly explain AHP shortening in small axotomized neurons [80]. The magnitude of current reduction was less in adjacent L4 neurons, and thus might be inadequate to exert an effect on AHP on the latter neurons. Because BK currents have also been implicated in limiting repetitive firing in small DRG neurons, their loss by axotomy may explain increased pain generation in neuropathic states.

Finally, considering the changes we observed as a result of SNL in axotomized and adjacent DRG neurons, dissociated from rats exhibiting hyperalgesic behavior after SNL, only comparison with neurons dissociated from rats subjected to the same treatment (SNL) but not responding with hyperalgesia to sensory testing would indicate whether these changes are pertinent in mediating hyperalgesic responses. Thus, non-responding rats after SNL would be appropriate to serve as an additional, pathophysiologically pertinent control group, the lack of which constitutes another limitation of our study.

An unexpected finding in our study is the lack of changes of I_{Na} after axotomy, in contrast to other reports of injury models in rodents [93,94]. The way we estimated Na^+ current by subtraction of the current after replacement of Na^+ with NMDG and blockade of TTX-sensitive channels determines the total inward I_{Na} via all Na^+ channel subtypes. Other studies have shown that axotomy decreases expression of some sodium channel subtypes but up-regulates others [8,46,76]. Thus, injury-related effects on different subtypes might negate or counterbalance each other, resulting in minimal total I_{Na} change.

Our experimental approach does not provide mechanistic insights to explain the changes in $I_{K(Ca)}$ we have observed, other than the recognition that these are independent of any I_{Ca} alterations. However, it has been shown that neuronal $K_{(Ca)}$ channels are highly dependent on trophic factors, such as NGF and NT3. Nerve growth factor application increases the expression of $K_{(Ca)}$ channels in cultured rat DRG cells [7], and NT3 stimulates human IK expression [7]. Furthermore, NGF and NT3 activate BK channels in rodent brain [36]. Axotomy from SNL may deprive L5 neurons of trophic support necessary to maintain $I_{K(Ca)}$, whereas elevated NGF found in L4 DRGs after SNL [19] may promote greater than normal expression of $I_{K(Ca)}$, as observed in this study.

The recognition of dysregulation of $K_{(Ca)}$ channels after injury of primary afferent neurons may provide the opportunity for pharmacological manipulations in neuropathic pain after peripheral nerve injury, using appropriate channel activators or modulators delivered to specific DRG. For instance, decreased neuronal excitability may be expected after application of the SK channel openers 1-ethyl-2-benzimidazolinone (1-EBIO) [4] and chlorzoxazone [10,89], the SK and IK opener (E)-2-(4,6-difluoro-1-indanylidene) acetamide [65,66], or the selective BK opener benzimidazolone NS1619 [102].

Ethanol also directly activates neuronal large conductance $K_{(Ca)}$ channels in a reversible and dose-dependent manner [16]. Ethanol at clinically relevant concentrations, shortens AP, prolongs refractory period and decreases firing frequency in a subgroup of primary afferent neurons, most likely nociceptors, by activation of BK $K_{(Ca)}$ channels [27]. Thus, modulation of sensory information in primary afferent neurons may explain partly the analgesic and anesthetic effect of ethanol [43,95]. Similarly, the anesthetic and analgesic effects of chloral hydrate can be partly explained by the 20-fold more potent than ethanol activating effect of its active metabolite 2,2,2-trichloroethanol (TCE) on BK channels of DRG neurons, which results in a significant outward current and AP shortening with subsequent excitability reduction [26].

Experimental procedures

All procedures were approved by the Animal Care Committee of the Medical College of Wisconsin, Milwaukee, Wisconsin.

Experimental Neuropathic Injury Model

Male Sprague-Dawley rats (Taconic Farms Inc., Hudson, NY), 6 weeks old and weighing 125–160 g were randomly subjected to surgical axotomy using the SNL model, or to sham skin operation. The latter constituted the control group. Spinal nerve ligation was performed similar to the original description [47]. Briefly, animals were anesthetized with halothane (2–3%) in oxygen, and after lumbar incision the right lumbar paravertebral region was exposed, and the inter-transverse fascia was opened. The L6 transverse process was excised, and subsequently both the right fifth and the sixth lumbar spinal nerves were tightly ligated with 6-0 silk suture and transected distal to the ligature. The lumbar fascia was closed by 4-0 resorbable polyglactin suture, and the skin with three staples. In control rats, sham operation was performed by lumbar skin incision and closure only.

Sensory Testing

Selection of rats suitable for further tissue harvesting was performed after behavioral testing as previously described [33]. In order to become familiar with the testing procedures and environment, rats were brought to the testing area for 4 hours or more, at least one day after arrival at the animal care facility. Rats were tested on the 10th, 12th, and 14th postoperative days, on a 0.25 in. wire grid in clear plastic enclosures, after they had been allowed to rest for 30min. Sensory testing was performed by stimulating the plantar skin of hind paws in random order with a 22-gauge spinal needle applied with pressure adequate to indent but not penetrate the plantar skin. Five needle applications were delivered and repeated 3 min later. These mechanical stimuli produced either a normal brief flinch or withdrawal, or a response characterized by a sustained (> 2 s) paw lifting, shaking and licking. SNL animals that displayed a hyperalgesia-type response (sustained lifting, licking, chewing, or shaking of the paw) were considered to express a phenotype of neuropathic pain, whereas others without hyperalgesic responses were considered to lack neuropathic pain. Only SNL rats with an ipsilateral hyperalgesic response (at least 20% averaged over 3 test days) and normal contralateral responses, as well as SS rats with normal bilateral responses were used for study. Hyperalgesic

response rates were calculated as described previously [33], and compared between SNL-operated and skin sham operated rats that were included in the study by Mann-Whitney non-parametric test.

Cell Isolation and Plating

One hundred and forty four neurons were studied. The L4 and L5 DRG were removed from control, as well as from hyperalgesic rats, two to three weeks after SNL injury or sham skin operation. Animals were sacrificed by decapitation under halothane anesthesia. DRGs were removed through a lumbar incision, placed into separate 35 mm Petri dishes containing cold, oxygenated, calcium- and magnesium chloride-free Hanks Balanced Salt Solution, and minced with iris scissors. Minced ganglia were subsequently enzymatically dissociated in a solution containing 0.0625% trypsin (Boehringer-Mannheim), 0.0125% deoxyribonuclease 1 (Sigma, St. Louis, MO) and 0.0125% liberase blendzyme 2 (Roche Diagnostics Corp., Indianapolis, IN) in 4.5 ml DMEM/F12 (Dulbecco's modified Eagle's medium F12; Gibco, Carlsbad, CA) for 90 min in a shaker bath at 32°C and 70 rpm. Cells were isolated by centrifugation, re-suspended in a culture medium consisting of 0.5 mM glutamine, 0.02 mg/ml gentamicin, 100 ng/ml nerve growth factor 7S (Alomone Labs, Jerusalem, Israel), 2% (vol/vol) B-27 supplement (Life Technologies, Rockville, MD), and 98% (vol/vol) neural basal medium A 1X (Life Technologies), and finally plated onto two to four poly-l-lysine-coated 12-mm glass coverslips (Deutsche Spiegelglas; Carolina Biologic Supply, Burlington, NC) per ganglion. Cells were then incubated for 2–3 h in a humidified incubator at 37°C with 95% air and 5% CO_2 and were studied within 3–8 h of dissociation.

Recording Protocols

Neurons on cover slips were viewed with an inverted microscope (Nikon Diaphot 300) using Hoffman modulation optic systems. Electrophysiological recordings of medium sized neurons (30–39 μm in diameter) as well as of small neurons (<30 μm) were conducted at room temperature, in whole-cell patch configuration, initially in current clamp and then switching to voltage clamp mode (Axopatch 200B amplifier, Axon Instruments Inc., Union City, CA). Criteria for accepting neurons in the study were resting membrane potential equal or more negative than −45 mV, access resistance less than 10 MΩ, as well as absence of significant leak or appreciable rundown within the time frame of recordings.

All recordings were obtained at room temperature. Signals were acquired at 5 to 10 kHz (Digidata 1200B data acquisition board, Axon Instruments), and filtered through an 8-pole Bessel filter. The pClamp (Axon Instruments, Inc) Clampex version 9.2.0.10 was used for data acquisition, and Clampfit version 9.2.0.10 for data analysis.

Patch micropipette electrodes were pulled from borosilicate glass capillaries using a Flaming/Brown micropipette puller, model P-97 (Sutter, San Rafael, CA) and flame polished with a microforge polisher (Narishige, Tokyo) prior to use. Resistance of the internal solution filled pipettes, in the recording solutions, ranged from 2 to 4.5 MΩ. Access resistances before series resistance compensation were 4–8 MΩ. After the completion of the breakthrough process, cell capacitance and series resistance was compensated by 80–90% with the compensation circuitry of the amplifier.

Action potentials were triggered in current clamp mode with 2 ms current injection pulses of 1 to 5 nA. This was followed by a recording lasting 500 ms. Action potentials were recorded from each neuron in Tyrode's solution, and then replayed as voltage command stimuli in a time course mode, every 10s. Each individual cell's resting membrane potential and recorded AP waveform were used as the holding membrane potential and voltage command stimulus,

respectively, in the same neuron, in voltage clamp mode. Agents and solutions were applied by fluid changes under continuous perfusion through a gravity dependent flow system.

Apamin and iberiotoxin were diluted daily in the external solution from lyophilized stocks kept at −70°C, while clotrimazole from 10 mM stocks in DMSO kept at 4°C. These toxins, as well as glibenclamide, were obtained from Sigma, St. Louis, MO. In these protocols the Tyrode's solution, consisted of the following (in mM): 140 NaCl, 4 KCl, 2 $CaCl_2$, 2 $MgCl_2$, 10 D-glucose, 10 HEPES, at pH of 7.4 buffered with NaOH and an osmolarity of 300 mOsm. For the protocols employing AP recordings and stimulation by AP waveform voltage commands, internal pipette solution contained (in mM) 120 KCl, 5 Na-ATP, 0.4 Na-GTP, 5 EGTA, 2.25 $CaCl_2$, 5 $MgCl_2$, 20 HEPES, at a pH of 7.4 buffered with KOH and osmolarity of 296–300 mOsm ("regular internal pipette solution for AP recordings").

Current was normalized by membrane capacitance, yielding current density corrected for cell size. Na^+ current component was estimated by subtracting the current density recorded in NMDG/TTX Tyrode's from the baseline current in regular Tyrode's. Current sensitive to $K_{(Ca)}$ blockers ($I_{K(Ca)}$) was derived as a difference current by subtracting the new current recorded after administration of the combined $K_{(Ca)}$ blockers from the current recorded in NMDG/TTX Tyrode's, while total K^+ current ($I_{K(tot)}$) was assumed to be that resulting after subtracting the current after the addition of all K^+ channel blockers (1 mM 4-AP, 160 mM TEA-Cl and 1 μM glibenclamide in addition to $K_{(Ca)}$ blockers) from the current in NMDG/TTX Tyrode's. With this protocol, we were able to measure I_{Na}, $I_{K(Ca)}$, total I_K ($I_{K(tot)}$,), and I_{Ca} in the same cell. Peak inward current (for current components sensitive to Na^+ and Ca^{2+} influx blockade), peak outward current (for K^+ currents sensitive to $K_{(Ca)}$ blockers alone, and together with 4-AP, TEA-Cl and glibenclamide), as well as corresponding total charge transfer (current integrated over time) were determined digitally.

4-AP blocks delayed rectifier and A-type potassium channels [32] (IC_{50} 1–2 mM for various neuronal K+ channels [18,79,84]), glibenclamide selectively blocks ATP-sensitive K^+ channels [32] (IC_{50} for inhibition of levcromakalim-activated current in adult rat intracardiac ganglionic neurons 55 nM [35]), and TEA blocks delayed rectifier, inward rectifier, A-type, BK and ATP-sensitive K^+ channels [32] (IC_{50} in the low mM range for voltage-gated K+ currents in neurons [49], or in the 1–100 mM range for blocking various neuronal K^+ channels [41,67]).

In other experiments, currents were recorded using pipette solution dialyzing the cytosol with calculated final free $[Ca^{2+}]_i$ clamped at 1μM. The external solution used in these experiments contained 140 NaCl, 3 KCl, 1 $CaCl_2$, 1 $MgCl_2$, 10 D-glucose, 10 HEPES, 0.1 μM TTX, 1 μM glibenclamide, 1 4-AP and 200 μM cadmium at pH of 7.4 buffered with NaOH and an osmolarity of 300 mOsm. We included a low concentration of $CaCl_2$ in order to avoid any contaminating effects from Ca^{2+} ions present in the external solution, and we preferred to inhibit influx via VGCC with cadmium. 4-AP and glibenclamide were included to block contamination from other potassium current subtypes [82]. Internal pipette solution for the second set of experiments contained (in mM) 10 KCl, 110 potassium gluconate, 5 NaCl, 5 Na-ATP, 2 $MgCl_2$, 0.2 Na-GTP, 2 EGTA, 1.8 $CaCl_2$, 10 HEPES, at a pH of 7.4 buffered with KOH and osmolarity of 296–300 mOsm ("internal pipette solution with Ca^{2+} clamped at 1 mM").

We calculated the free Ca^{2+} concentration using a free Ca^{2+} concentration calculator software program, available online at http://entropy.brneurosci.org/cgi-bin/egta. Calculations are based on a previous publication by Portzehl et al [71]. Based on this calculator, concentrations of Ca^{2+} and Mg^{2+} ions and buffer were adjusted so that free Ca^{2+} ions concentration would be approximately 1 μM.

Current rundown was absent or minimal in most cells during our recordings. Actual current traces were selected for further analysis either before or subsequent to administration of new solutions containing blockers or toxins, after we confirmed that currents had been stabilized to a steady-state level and subsequently remained stable over time. In the first set of experiments utilizing AP waveform stimuli, recordings were conducted in a time course mode, in which stability became directly evident before and after the blocker effect took place. With regard to the second set of experiments (using square voltage commands and specific toxins), we obtained serial current recordings, recorded at intervals. We confirmed significant stability of the amplitude of current traces over time at baseline, and administration of the toxin containing solutions did not commence unless such current stability at baseline was confirmed. We also confirmed that current amplitudes stabilized at a new steady state after the action of the toxin administered, after which remained stable over time as well. Neurons exhibiting any evidence of significant current rundown were rejected from the study.

Measured inward current was normalized by membrane capacitance, which results in a current density corrected for cell size. Apamin-, clotrimazole-, or iberiotoxin-sensitive current components were determined by subtracting toxin-induced from baseline current densities. These toxins were applied in different cells each, and only one at a time to avoid problems with incomplete washout. Current-voltage relationship curves were plotted from the subtracted currents and averaged for each neuronal subtype.

Statistical Analyses

Cells were categorized according to surgical preparation. Neurons were grouped according to surgical preparation and DRG level into control (from SS rats), axotomized neurons from the L5 DRG after SNL, and neurons from the L4 DRG after SNL (adjacent to injury). Since there were no differences in responses from L4 and L5 ganglia from control rats, these cells were combined. Data were analyzed with SPSS Version 11 for Macintosh OS X (SPSS, Inc). For each dependent variable, the main effect of a group was tested with either standard one-way ANOVA or the Univariate General Linear Model ANOVA function of the SPSS, unless indicated otherwise. Whenever one-way or Univariate ANOVA indicated statistical significance in identifying a significant main effect, post hoc comparisons between groups were tested in a pair-wise manner by LSD post hoc tests. For example when a main effect was significant, post hoc comparisons were conducted: control versus L5 SNL, control versus L4 SNL, and L5 SNL versus L4 SNL.

In determining if toxins blocked a current to a significant degree, the current reduction was estimated by subtracting the trace after the administration of the toxin from the preceding baseline trace. For each individual neuron we used the peak current density values (current normalized for each individual cell's capacitance) at each membrane potential cell. To check if the currents after the toxins differed from the currents at baseline we used Univariate ANOVA examining the toxin effect as an independent main effect. Data are presented as means±SE in the text and the figures, unless stated otherwise.

References

1. Abdulla FA, Smith PA. Axotomy- and autotomy-induced changes in Ca2+ and K+ channel currents of rat dorsal root ganglion neurons. J Neurophysiol 2001;85:644–658. [PubMed: 11160500]
2. Akins PT, McCleskey EW. Characterization of potassium currents in adult rat sensory neurons and modulation by opioids and cyclic AMP. Neuroscience 1993;56:759–769. [PubMed: 8255432]
3. Amir R, Devor M. Spike-evoked suppression and burst patterning in dorsal root ganglion neurons of the rat. J Physiol 1997;501(Pt 1):183–196. [PubMed: 9175002]

4. Bahia PK, Suzuki R, Benton DC, Jowett AJ, Chen MX, Trezise DJ, Dickenson AH, Moss GW. A functional role for small-conductance calcium-activated potassium channels in sensory pathways including nociceptive processes. J Neurosci 2005;25:3489–3498. [PubMed: 15814779]
5. Berridge MJ, Lipp P, Bootman MD. The versatility and universality of calcium signalling. Nat Rev Mol Cell Biol 2000;1:11–21. [PubMed: 11413485]
6. Blenk KH, Habler HJ, Janig W. Neomycin and gadolinium applied to an L5 spinal nerve lesion prevent mechanical allodynia-like behaviour in rats. Pain 1997;70:155–165. [PubMed: 9150289]
7. Boettger MK, Till S, Chen MX, Anand U, Otto WR, Plumpton C, Trezise DJ, Tate SN, Bountra C, Coward K, Birch R, Anand P. Calcium-activated potassium channel SK1- and IK1-like immunoreactivity in injured human sensory neurones and its regulation by neurotrophic factors. Brain 2002;125:252–263. [PubMed: 11844726]
8. Boucher TJ, Okuse K, Bennett DL, Munson JB, Wood JN, McMahon SB. Potent analgesic effects of GDNF in neuropathic pain states. Science 2000;290:124–127. [PubMed: 11021795]
9. Bouhassira D, Attal N, Willer JC, Brasseur L. Painful and painless peripheral sensory neuropathies due to HIV infection: a comparison using quantitative sensory evaluation. Pain 1999;80:265–272. [PubMed: 10204739]
10. Cao Y, Dreixler JC, Roizen JD, Roberts MT, Houamed KM. Modulation of recombinant small-conductance Ca(2+)-activated K(+) channels by the muscle relaxant chlorzoxazone and structurally related compounds. J Pharmacol Exp Ther 2001;296:683–689. [PubMed: 11181893]
11. Chung JM, Chung K. Importance of hyperexcitability of DRG neurons in neuropathic pain. Pain Practice 2002;2:87–97. [PubMed: 17147683]
12. Dallman JE, Dorman JB, Moody WJ. Action potential waveform voltage clamp shows significance of different Ca2+ channel types in developing ascidian muscle. J Physiol 2000;524(Pt 2):375–386. [PubMed: 10766919]
13. Devor M, Govrin-Lippmann R, Frank I, Raber P. Proliferation of primary sensory neurons in adult rat dorsal root ganglion and the kinetics of retrograde cell loss after sciatic nerve section. Somatosens Res 1985;3:139–167. [PubMed: 3835669]
14. Devor M, Janig W, Michaelis M. Modulation of activity in dorsal root ganglion neurons by sympathetic activation in nerve-injured rats. J Neurophysiol 1994;71:38–47. [PubMed: 8158237]
15. Devor M, Wall PD. Cross-excitation in dorsal root ganglia of nerve-injured and intact rats. J Neurophysiol 1990;64:1733–1746. [PubMed: 2074461]
16. Dopico AM, Lemos JR, Treistman SN. Ethanol increases the activity of large conductance, Ca(2+)-activated K+ channels in isolated neurohypophysial terminals. Mol Pharmacol 1996;49:40–48. [PubMed: 8569710]
17. Faber ES, Sah P. Calcium-activated potassium channels: multiple contributions to neuronal function. Neuroscientist 2003;9:181–194. [PubMed: 15065814]
18. Foehring RC, Surmeier DJ. Voltage-gated potassium currents in acutely dissociated rat cortical neurons. J Neurophysiol 1993;70:51–63. [PubMed: 8395588]
19. Fukuoka T, Kondo E, Dai Y, Hashimoto N, Noguchi K. Brain-derived neurotrophic factor increases in the uninjured dorsal root ganglion neurons in selective spinal nerve ligation model. J Neurosci 2001;21:4891–4900. [PubMed: 11425916]
20. Fukuoka T, Tokunaga A, Tachibana T, Dai Y, Yamanaka H, Noguchi K. VR1, but not P2X(3), increases in the spared L4 DRG in rats with L5 spinal nerve ligation. Pain 2002;99:111–120. [PubMed: 12237189]
21. Gabso M, Neher E, Spira ME. Low mobility of the Ca2+ buffers in axons of cultured Aplysia neurons. Neuron 1997;18:473–481. [PubMed: 9115740]
22. Garcia ML, Hanner M, Knaus HG, Koch R, Schmalhofer W, Slaughter RS, Kaczorowski GJ. Pharmacology of potassium channels. Adv Pharmacol 1997;39:425–471. [PubMed: 9160122]
23. Gold MS. Spinal nerve ligation: what to blame for the pain and why. Pain 2000;84:117–120. [PubMed: 10666515]
24. Gold MS, Shuster MJ, Levine JD. Role of a Ca(2+)-dependent slow afterhyperpolarization in prostaglandin E2-induced sensitization of cultured rat sensory neurons. Neurosci Lett 1996;205:161–164. [PubMed: 8852583]

25. Govrin-Lippmann R, Devor M. Ongoing activity in severed nerves: source and variation with time. Brain Res 1978;159:406–410. [PubMed: 215270]
26. Gruss M, Hempelmann G, Scholz A. Trichloroethanol alters action potentials in a subgroup of primary sensory neurones. Neuroreport 2002;13:853–856. [PubMed: 11997700]
27. Gruss M, Henrich M, Konig P, Hempelmann G, Vogel W, Scholz A. Ethanol reduces excitability in a subgroup of primary sensory neurons by activation of BK(Ca) channels. Eur J Neurosci 2001;14:1246–1256. [PubMed: 11703454]
28. Hamill OP, Marty A, Neher E, Sakmann B, Sigworth FJ. Improved patch-clamp techniques for high-resolution current recording from cells and cell-free membrane patches. Pflugers Arch 1981;391:85–100. [PubMed: 6270629]
29. Hanselmann C, Grissmer S. Characterization of apamin-sensitive Ca(2+)-activated potassium channels in human leukaemic T lymphocytes. J Physiol 1996;496(Pt 3):627–637. [PubMed: 8930831]
30. Hay M, Kunze DL. An intermediate conductance calcium-activated potassium channel in rat visceral sensory afferent neurons. Neurosci Lett 1994;167:179–182. [PubMed: 7513840]
31. Herrera GM, Nelson MT. Differential regulation of SK and BK channels by Ca(2+) signals from Ca (2+) channels and ryanodine receptors in guinea-pig urinary bladder myocytes. J Physiol 2002;541:483–492. [PubMed: 12042353]
32. Hille, B. Potassium channels and chloride channels. In: Hille, B., editor. Ion channels of excitable membranes. Sinauer Associates, Inc; Sunderland, Massachusets: 2001. p. 131-167.
33. Hogan Q, Sapunar D, Modric-Jednacak K, McCallum JB. Detection of neuropathic pain in a rat model of peripheral nerve injury. Anesthesiology 2004;101:476–487. [PubMed: 15277932]
34. Hogan QH, McCallum JB, Sarantopoulos C, Aason M, Mynlieff M, Kwok WM, Bosnjak ZJ. Painful neuropathy decreases membrane calcium current in mammalian primary afferent neurons. Pain 2000;86:43–53. [PubMed: 10779659]
35. Hogg RC, Adams DJ. An ATP-sensitive K(+) conductance in dissociated neurones from adult rat intracardiac ganglia. Journal of Physiology 2001;534:713–720. [PubMed: 11483702]
36. Holm NR, Christophersen P, Olesen SP, Gammeltoft S. Activation of calcium-dependent potassium channels in mouse [correction of rat] brain neurons by neurotrophin-3 and nerve growth factor. Proc Natl Acad Sci U S A 1997;94:1002–1006. [PubMed: 9023372]
37. Honma Y, Yamakage M, Ninomiya T. Effects of adrenergic stimulus on the activities of Ca2+ and K+ channels of dorsal root ganglion neurons in a neuropathic pain model. Brain Res 1999;832:195–206. [PubMed: 10375670]
38. Hu H, Shao LR, Chavoshy S, Gu N, Trieb M, Behrens R, Laake P, Pongs O, Knaus HG, Ottersen OP, Storm JF. Presynaptic Ca2+-activated K+ channels in glutamatergic hippocampal terminals and their role in spike repolarization and regulation of transmitter release. J Neurosci 2001;21:9585–9597. [PubMed: 11739569]
39. Huang LY, Neher E. Ca(2+)-dependent exocytosis in the somata of dorsal root ganglion neurons. Neuron 1996;17:135–145. [PubMed: 8755485]
40. Hudson LJ, Bevan S, Wotherspoon G, Gentry C, Fox A, Winter J. VR1 protein expression increases in undamaged DRG neurons after partial nerve injury. Eur J Neurosci 2001;13:2105–2114. [PubMed: 11422451]
41. Huguenard JR, Prince DA. Slow inactivation of a TEA-sensitive K current in acutely isolated rat thalamic relay neurons. J Neurophysiol 1991;66:1316–1328. [PubMed: 1761985]
42. Ishii TM, Silvia C, Hirschberg B, Bond CT, Adelman JP, Maylie J. A human intermediate conductance calcium-activated potassium channel. Proc Natl Acad Sci U S A 1997;94:11651–11656. [PubMed: 9326665]
43. James MF, Duthie AM, Duffy BL, McKeag AM, Rice CP. Analgesic effect of ethyl alcohol. Br J Anaesth 1978;50:139–141. [PubMed: 341934]
44. Jensen BS, Strobaek D, Christophersen P, Jorgensen TD, Hansen C, Silahtaroglu A, Olesen SP, Ahring PK. Characterization of the cloned human intermediate-conductance Ca2+-activated K+ channel. Am J Physiol 1998;275:C848–856. [PubMed: 9730970]

45. Kajander KC, Wakisaka S, Bennett GJ. Spontaneous discharge originates in the dorsal root ganglion at the onset of a painful peripheral neuropathy in the rat. Neuroscience Letters 1992;138:225–228. [PubMed: 1319012]
46. Kim CH, Oh Y, Chung JM, Chung K. The changes in expression of three subtypes of TTX sensitive sodium channels in sensory neurons after spinal nerve ligation. Brain Res Mol Brain Res 2001;95:153–161. [PubMed: 11687287]
47. Kim SH, Chung JM. An experimental model for peripheral neuropathy produced by segmental spinal nerve ligation in the rat. Pain 1992;50:355–363. [PubMed: 1333581]
48. Kingery WS. A critical review of controlled clinical trials for peripheral neuropathic pain and complex regional pain syndromes. Pain 1997;73:123–139. [PubMed: 9415498]
49. Klee R, Ficker E, Heinemann U. Comparison of voltage-dependent potassium currents in rat pyramidal neurons acutely isolated from hippocampal regions CA1 and CA3. J Neurophysiol 1995;74:1982–1995. [PubMed: 8592191]
50. Lawson SN. Phenotype and function of somatic primary afferent nociceptive neurones with C-, Adelta- or Aalpha/beta-fibres. Exp Physiol 2002;87:239–244. [PubMed: 11856969]
51. Leung A, Wallace MS, Ridgeway B, Yaksh T. Concentration-effect relationship of intravenous alfentanil and ketamine on peripheral neurosensory thresholds, allodynia and hyperalgesia of neuropathic pain. Pain 2001;91:177–187. [PubMed: 11240090]
52. Lewis SE, Mannion RJ, White FA, Coggeshall RE, Beggs S, Costigan M, Martin JL, Dillmann WH, Woolf CJ. A role for HSP27 in sensory neuron survival. J Neurosci 1999;19:8945–8953. [PubMed: 10516313]
53. Liu CN, Wall PD, Ben-Dor E, Michaelis M, Amir R, Devor M. Tactile allodynia in the absence of C-fiber activation: altered firing properties of DRG neurons following spinal nerve injury. Pain 2000;85:503–521. [PubMed: 10781925]
54. Liu X, Chang Y, Reinhart PH, Sontheimer H, Chang Y. Cloning and characterization of glioma BK, a novel BK channel isoform highly expressed in human glioma cells. J Neurosci 2002;22:1840–1849. [PubMed: 11880513]
55. Liu X, Chung K, Chung JM. Ectopic discharges and adrenergic sensitivity of sensory neurons after spinal nerve injury. Brain Res 1999;849:244–247. [PubMed: 10592310]
56. Liu X, Eschenfelder S, Blenk KH, Janig W, Habler H. Spontaneous activity of axotomized afferent neurons after L5 spinal nerve injury in rats. Pain 2000;84:309–318. [PubMed: 10666536]
57. Luscher C, Streit J, Lipp P, Luscher HR. Action potential propagation through embryonic dorsal root ganglion cells in culture. II. Decrease of conduction reliability during repetitive stimulation. J Neurophysiol 1994;72:634–643. [PubMed: 7983525]
58. Ma C, Shu Y, Zheng Z, Chen Y, Yao H, Greenquist KW, White FA, LaMotte RH. Similar electrophysiological changes in axotomized and neighboring intact dorsal root ganglion neurons. J Neurophysiol 2003;89:1588–1602. [PubMed: 12612024]
59. Magistretti J, Mantegazza M, Guatteo E, Wanke E. Action potentials recorded with patch-clamp amplifiers: are they genuine? Trends Neurosci 1996;19:530–534. [PubMed: 8961481]
60. McCallum JB, Kwok WM, Mynlieff M, Bosnjak ZJ, Hogan QH. Loss of T-type calcium current in sensory neurons of rats with neuropathic pain. Anesthesiology 2003;98:209–216. [PubMed: 12502999]
61. McCallum JB, Kwok WM, Sapunar D, Fuchs A, Hogan QH. Painful peripheral nerve injury decreases calcium current in axotomized sensory neurons. Anesthesiology 2006;105:160–168. [PubMed: 16810008]
62. McCobb DP, Beam KG. Action potential waveform voltage-clamp commands reveal striking differences in calcium entry via low and high voltage-activated calcium channels. Neuron 1991;7:119–127. [PubMed: 1648936]
63. Moon DE, Lee DH, Han HC, Xie J, Coggeshall RE, Chung JM. Adrenergic sensitivity of the sensory receptors modulating mechanical allodynia in a rat neuropathic pain model. Pain 1999;80:589–595. [PubMed: 10342420]
64. Moore S, Thanos S. Differential increases in rat retinal ganglion cell size with various methods of optic nerve lesion. Neurosci Lett 1996;207:117–120. [PubMed: 8731435]

65. Musso DL, Cochran FR, Kelley JL, McLean EW, Selph JL, Rigdon GC, Orr GF, Davis RG, Cooper BR, Styles VL, Thompson JB, Hall WR. Indanylidenes. 1. Design and synthesis of (E)-2-(4,6-difluoro-1-indanylidene)acetamide, a potent, centrally acting muscle relaxant with antiinflammatory and analgesic activity. J Med Chem 2003;46:399–408. [PubMed: 12540239]
66. Musso DL, Orr GF, Cochran FR, Kelley JL, Selph JL, Rigdon GC, Cooper BR, Jones ML. Indanylidenes. 2. Design and synthesis of (E)-2-(4-chloro-6-fluoro-1-indanylidene)-N-methylacetamide, a potent antiinflammatory and analgesic agent without centrally acting muscle relaxant activity. J Med Chem 2003;46:409–416. [PubMed: 12540240]
67. Nisenbaum ES, Wilson CJ, Foehring RC, Surmeier DJ. Isolation and characterization of a persistent potassium current in neostriatal neurons. J Neurophysiol 1996;76:1180–1194. [PubMed: 8871229]
68. Nordin M, Nystrom B, Wallin U, Hagbarth KE. Ectopic sensory discharges and paresthesiae in patients with disorders of peripheral nerves, dorsal roots and dorsal columns. Pain 1984;20:231–245. [PubMed: 6096790]
69. Petersen M, Eckert AS, Segond von Banchet G, Heppelmann B, Klusch A, Kniffki KD. Plasticity in the expression of bradykinin binding sites in sensory neurons after mechanical nerve injury. Neuroscience 1998;83:949–959. [PubMed: 9483576]
70. Petersen M, Zhang J, Zhang JM, LaMotte RH. Abnormal spontaneous activity and responses to norepinephrine in dissociated dorsal root ganglion cells after chronic nerve constriction. Pain 1996;67:391–397. [PubMed: 8951934]
71. Portzehl H, Caldwell PC, Rueegg JC. The Dependence of Contraction and Relaxation of Muscle Fibres from the Crab Maia Squinado on the Internal Concentration of Free Calcium Ions. Biochim Biophys Acta 1964;79:581–591. [PubMed: 14179458]
72. Raffaelli G, Saviane C, Mohajerani MH, Pedarzani P, Cherubini E. BK potassium channels control transmitter release at CA3-CA3 synapses in the rat hippocampus. J Physiol 2004;557:147–157. [PubMed: 15034127]
73. Rasmussen PV, Sindrup SH, Jensen TS, Bach FW. Symptoms and signs in patients with suspected neuropathic pain. Pain 2004;110:461–469. [PubMed: 15275799]
74. Ringkamp M, Meyer RA. Injured versus uninjured afferents: Who is to blame for neuropathic pain? Anesthesiology 2005;103:221–223. [PubMed: 16052101]
75. Robitaille R, Garcia ML, Kaczorowski GJ, Charlton MP. Functional colocalization of calcium and calcium-gated potassium channels in control of transmitter release. Neuron 1993;11:645–655. [PubMed: 7691106]
76. Rola R, Szulczyk PJ, Witkowski G. Voltage-dependent Ca2+ currents in rat cardiac dorsal root ganglion neurons. Brain Res 2003;961:171–178. [PubMed: 12535791]
77. Sah P, Davies P. Calcium-activated potassium currents in mammalian neurons. Clin Exp Pharmacol Physiol 2000;27:657–663. [PubMed: 10972528]
78. Sah P, Faber ES. Channels underlying neuronal calcium-activated potassium currents. Prog Neurobiol 2002;66:345–353. [PubMed: 12015199]
79. Saito Y, Isa T. Voltage-gated transient outward currents in neurons with different firing patterns in rat superior colliculus. J Physiol 2000;528(Pt 1):91–105. [PubMed: 11018108]
80. Sapunar D, Ljubkovic M, Lirk P, McCallum JB, Hogan QH. Distinct membrane effects of spinal nerve ligation on injured and adjacent dorsal root ganglion neurons in rats. Anesthesiology 2005;103:360–376. [PubMed: 16052119]
81. Sarantopoulos C, McCallum B, Kwok WM, Hogan Q. Gabapentin decreases membrane calcium currents in injured as well as in control mammalian primary afferent neurons. Reg Anesth Pain Med 2002;27:47–57. [PubMed: 11799505]
82. Sarantopoulos C, McCallum B, Sapunar D, Kwok WM, Hogan Q. ATP-sensitive potassium channels in rat primary afferent neurons: the effect of neuropathic injury and gabapentin. Neurosci Lett 2003;343:185–189. [PubMed: 12770693]
83. Scholz A, Gruss M, Vogel W. Properties and functions of calcium-activated K+ channels in small neurones of rat dorsal root ganglion studied in a thin slice preparation. J Physiol 1998;513(Pt 1):55–69. [PubMed: 9782159]
84. Segal M, Rogawski MA, Barker JL. A transient potassium conductance regulates the excitability of cultured hippocampal and spinal neurons. J Neurosci 1984;4:604–609. [PubMed: 6699688]

85. Sindrup SH, Jensen TS. Efficacy of pharmacological treatments of neuropathic pain: an update and effect related to mechanism of drug action. Pain 1999;83:389–400. [PubMed: 10568846]

86. Skinner LJ, Enee V, Beurg M, Jung HH, Ryan AF, Hafidi A, Aran JM, Dulon D. Contribution of BK Ca2+-activated K+ channels to auditory neurotransmission in the Guinea pig cochlea. J Neurophysiol 2003;90:320–332. [PubMed: 12611976]

87. Sun X, Gu XQ, Haddad GG. Calcium influx via L- and N-type calcium channels activates a transient large-conductance Ca2+-activated K+ current in mouse neocortical pyramidal neurons. J Neurosci 2003;23:3639–3648. [PubMed: 12736335]

88. Swett JE, Torigoe Y, Elie VR, Bourassa CM, Miller PG. Sensory neurons of the rat sciatic nerve. Exp Neurol 1991;114:82–103. [PubMed: 1915738]

89. Syme CA, Gerlach AC, Singh AK, Devor DC. Pharmacological activation of cloned intermediate- and small-conductance Ca(2+)-activated K(+) channels. Am J Physiol Cell Physiol 2000;278:C570–581. [PubMed: 10712246]

90. Vergara C, Latorre R, Marrion NV, Adelman JP. Calcium-activated potassium channels. Curr Opin Neurobiol 1998;8:321–329. [PubMed: 9687354]

91. Wall PD, Devor M. Sensory afferent impulses originate from dorsal root ganglia as well as from the periphery in normal and nerve injured rats. Pain 1983;17:321–339. [PubMed: 6664680]

92. Wanigasekara Y, Keast JR. Neurturin has multiple neurotrophic effects on adult rat sacral parasympathetic ganglion neurons. Eur J Neurosci 2005;22:595–604. [PubMed: 16101741]

93. Waxman SG, Cummins TR, Dib-Hajj S, Fjell J, Black JA. Sodium channels, excitability of primary sensory neurons, and the molecular basis of pain. Muscle Nerve 1999;22:1177–1187. [PubMed: 10454712]

94. Waxman SG, Dib-Hajj S, Cummins TR, Black JA. Sodium channels and pain. Proc Natl Acad Sci U S A 1999;96:7635–7639. [PubMed: 10393872]

95. Woodrow KM, Eltherington LG. Feeling no pain: alcohol as an analgesic. Pain 1988;32:159–163. [PubMed: 3362554]

96. Woolf CJ. Pain. Neurobiol Dis 2000;7:504–510. [PubMed: 11042064]

97. Woolf CJ, Mannion RJ. Neuropathic pain: aetiology, symptoms, mechanisms, and management. Lancet 1999;353:1959–1964. [PubMed: 10371588]

98. Wu G, Ringkamp M, Hartke TV, Murinson BB, Campbell JN, Griffin JW, Meyer RA. Early onset of spontaneous activity in uninjured C-fiber nociceptors after injury to neighboring nerve fibers. J Neurosci 2001;21:RC140. [PubMed: 11306646]

99. Xia XM, Fakler B, Rivard A, Wayman G, Johnson-Pais T, Keen JE, Ishii T, Hirschberg B, Bond CT, Lutsenko S, Maylie J, Adelman JP. Mechanism of calcium gating in small-conductance calcium-activated potassium channels. Nature 1998;395:503–507. [PubMed: 9774106]

100. Xing JL, Hu SJ. Relationship between calcium-dependent potassium channel and ectopic spontaneous discharges of injured dorsal root ganglion neurons in the rat. Brain Res 1999;838:218–221. [PubMed: 10446337]

101. Yip HK, Rich KM, Lampe PA, Johnson EM Jr. The effects of nerve growth factor and its antiserum on the postnatal development and survival after injury of sensory neurons in rat dorsal root ganglia. J Neurosci 1984;4:2986–2992. [PubMed: 6502217]

102. Zhang XF, Gopalakrishnan M, Shieh CC. Modulation of action potential firing by iberiotoxin and NS1619 in rat dorsal root ganglion neurons. Neuroscience 2003;122:1003–1011. [PubMed: 14643767]

103. Zimmermann M. Pathobiology of neuropathic pain. Eur J Pharmacol 2001;429:23–37. [PubMed: 11698024]

Abbreviations

($K_{(Ca)}$)
: Calcium-activated potassium

($I_{K(Ca)}$)
: calcium-activated potassium current

(AHP) after-hyperpolarization

($I_{(AHP)}$) current that mediates the medium and slow AHP

(HP) holding potential

(DRG) dorsal root ganglion

(L5) fifth lumbar

(L4) fourth lumbar

(SNL) spinal nerve ligation

(SK) small conductance potassium

(BK) large conductance potassium

(IK) intermediate conductance potassium

(SS) sham skin-operated

(NMDG) N-methyl-D-glucamine

(TTX) tetrodotoxin

(VGCC) voltage gated Ca^{2+} currents

(I_{Ca}) calcium influx or inward Ca^{2+} current

(AP) action potential

(4-AP) 4-aminopyridine

(TEA-Cl) tetraethylammonium chloride

(NGF) nerve growth factor

(NT3) neurotrophin-3

(EGTA)
ethylene glycol-bis (2-amino-ethylether)-N,N,N', N'-tetra-acetic acid

(AUC)
Area Under Curve

(I_{Na})
sodium current

(I_K)
potassium current

($I_{K(tot)}$)
"total" potassium current sensitive to apamine, iberiotoxin, clotrimazole, 4-AP, TEA-Cl, and glibenclamide

(n.s.)
not statistically significant

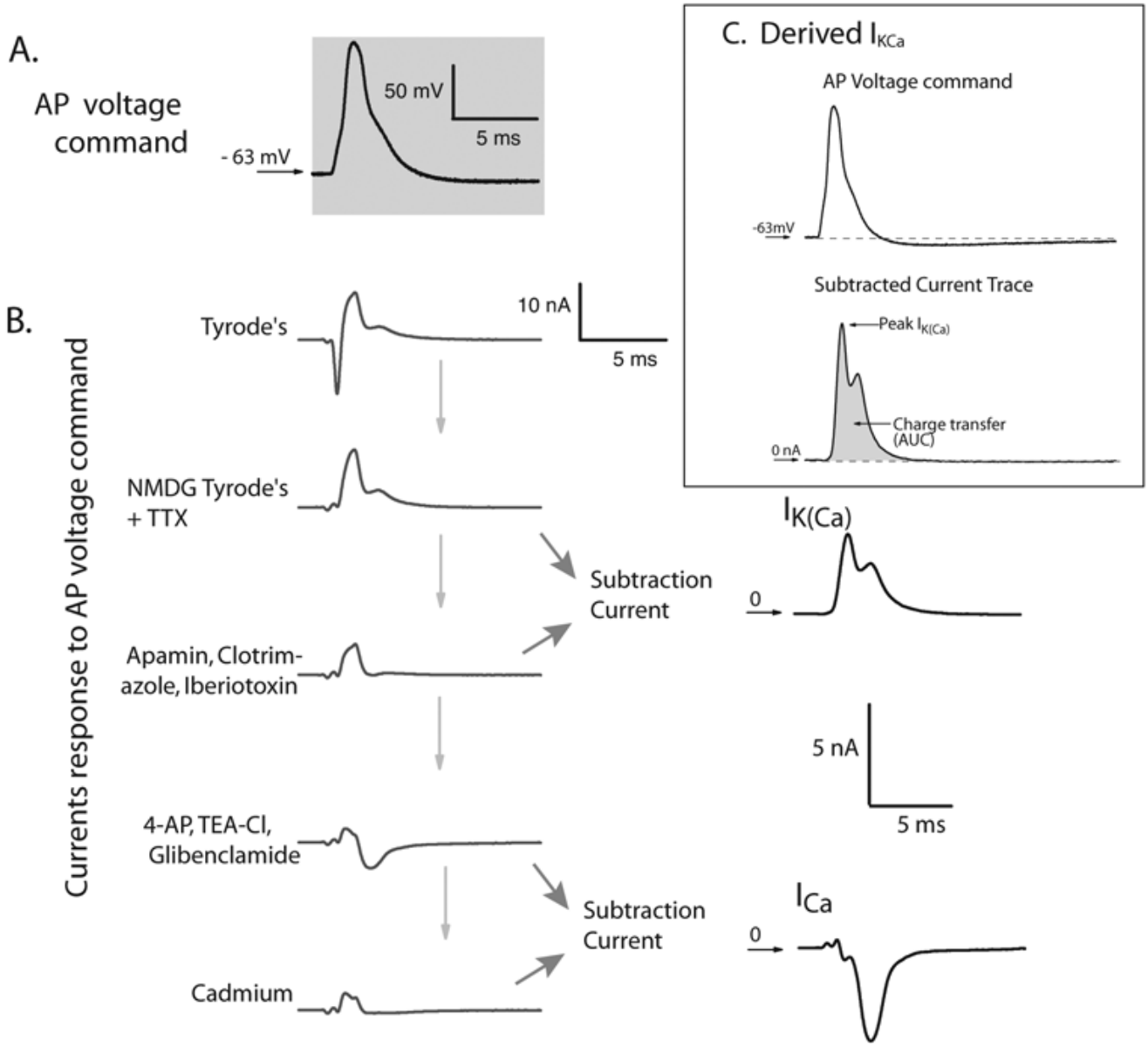

Figure 1.

Derivation of the difference current components attributable to I_{Na}, I_{Ca}, $I_{K(Ca)}$, and total I_K. A. AP recorded in current clamp mode and then replayed as voltage command stimulus in voltage clamp, from holding potential equal to this cell's resting membrane potential. B. Whole-cell currents in response to the AP voltage command in Tyrode's solution, and then sequentially after blocking I_{Na} with equimolar NMDG and 0.3μM TTX, after blocking $I_{K(Ca)}$ with apamin, iberiotoxin, and clotrimazole in combination, then after blocking remaining K^+ current with the addition of 4-AP, TEA-Cl, and glibenclamide, and finally blocking I_{Ca} with cadmium. All recordings were obtained sequentially from the same cell, using this individual cell's AP as voltage command stimulus. Individual current components were derived as difference currents by subtraction of the trace after administration of the blocker from the current trace before. Total I_K ($I_{K(tot)}$) was estimated as the potassium current sensitive to all the potassium channel blockers that we used (4-AP, TEA-Cl and glibenclamide in addition to apamin, iberiotoxin and

clotrimazole). This current was calculated by subtracting the current trace obtained after the addition of all these blockers, from the current recorded in the NMDG-containing Tyrode's solution. C. Derived potassium current ($I_{K(Ca)}$) sensitive to $K_{(Ca)}$ blockers (apamin, clotrimazole and iberiotoxin combined) in response to AP voltage command. Upper trace: AP recorded in current clamp mode and then replayed as voltage command stimulus in voltage clamp, from holding potential equal to this cell's resting membrane potential (also shown in A). Lower trace: Subtracted current trace, indicative of the derived $K_{(Ca)}$ current component, obtained as the difference between the current after administration of combined $K_{(Ca)}$ blockers, and baseline current in Tyrode's solution containing NMDG and TTX. Peak current as well as charge transfer (AUC) were derived digitally from this trace. Note that the peak $I_{(KCa)}$ occurs during the descending limb of the AP waveform command.

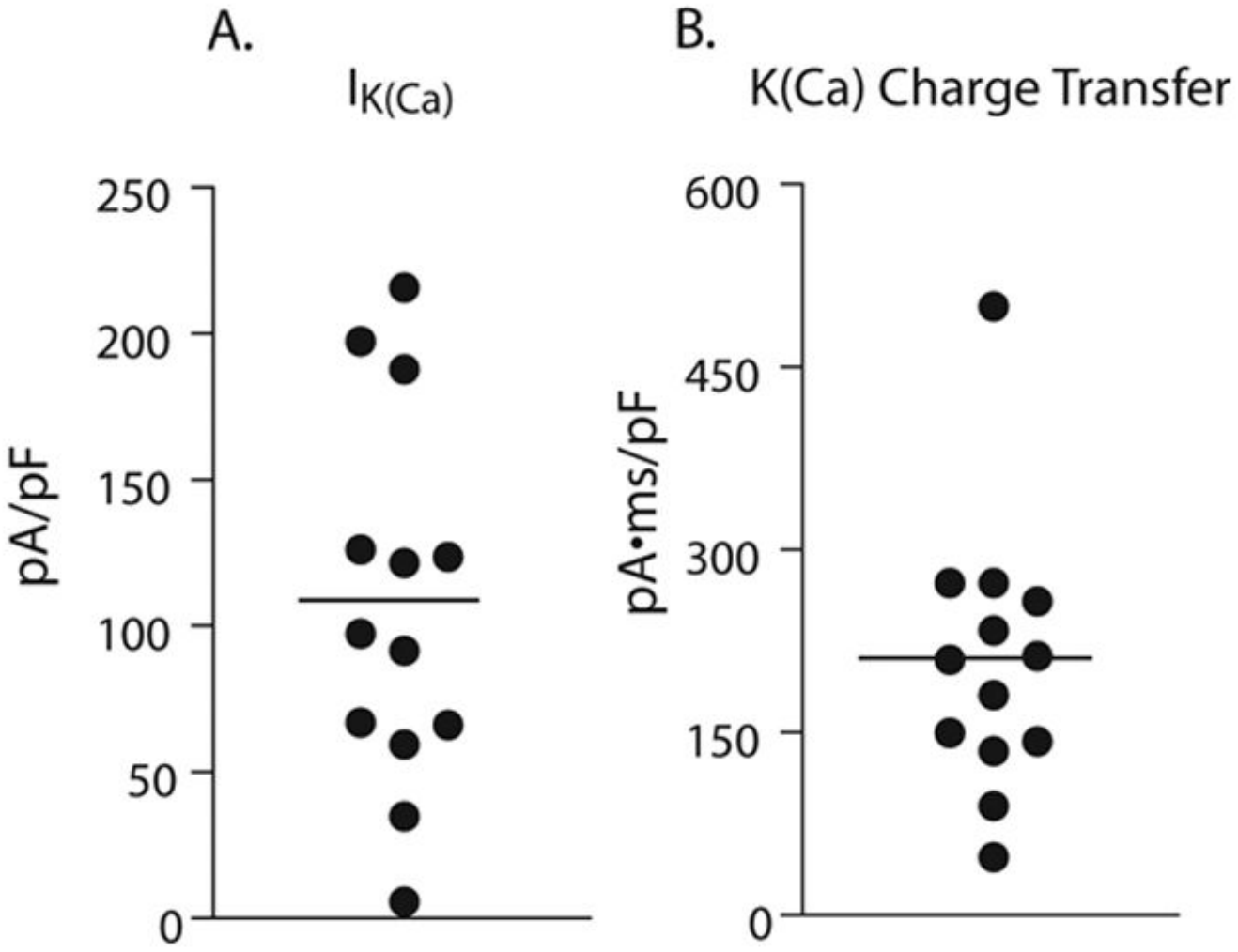

Figure 2.
Peak current values (A) and charge transfer values (B) for potassium current sensitive to apamin, iberiotoxin and clotrimazole combined, in control neuronal somata (n=13).

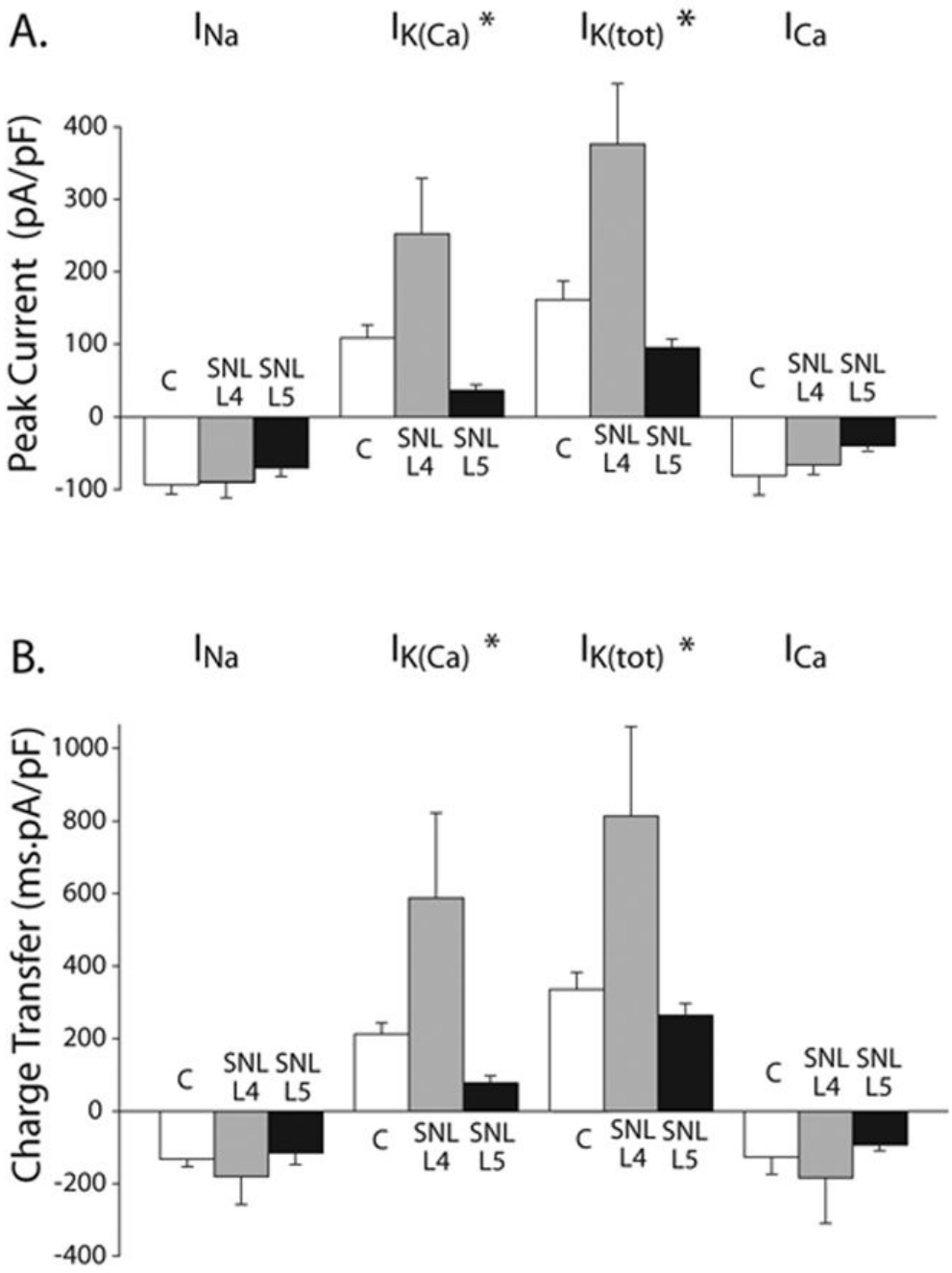

Figure 3.

Peak current (A), and charge transfer as estimated from the AUC (B), for difference current components attributable to I_{Na}, I_{Ca}, $I_{K(Ca)}$, and $I_{K(tot)}$, in medium-sized control neurons (C, n=13), as well as in axotomized (L5 SNL, n=14) or adjacent neurons (L4 SNL, n=14). AP waveforms were recorded in each cell in current-clamp and replayed as voltage commands to elicit currents in voltage-clamp sequentially in a time course mode. Difference currents were derived by subtraction of traces recorded by sequential application of blockers selective for each current component (see Figure 1). Peak current densities and charge transfer values were measured for each separate difference current after normalization by dividing by each cell's capacitance. Means ± SE are shown.

*: indicate statistically significant differences with regard to cell-type main effect.

I_{Na} peak current and charge transfer values did not differ among control, axotomized and adjacent neuronal somata. I_{Ca} peak current and charge transfer also did not differ between the three cell types. However, there were statistically significant differences for peak $I_{K(Ca)}$ currents and charge transfer values among different cell types (p=0.005 for peak current and p=0.029 for charge transfer), as well as for total I_K peak currents (p=0.001) and charge transfer (0.020). Post hoc analysis showed a statistically significant difference for peak $I_{K(Ca)}$ between L5 SNL and L4 SNL (p=0.001), and between control and L4 SNL (p=0.031). There was also a statistically significant difference for $I_{K(Ca)}$ charge transfer between L5 SNL and L4 SNL (p=0.01), as well as a marginal difference between control and L4 SNL (p=0.057). Peak total I_K also differed between L5 SNL and L4 SNL (p<0.001), and between control and L4 SNL (p=0.005). There was also a statistically significant difference for $I_{K(Ca)}$ charge transfer between L5 SNL and L4 SNL (p=0.009), as well as between control and L4 SNL (p=0.025).

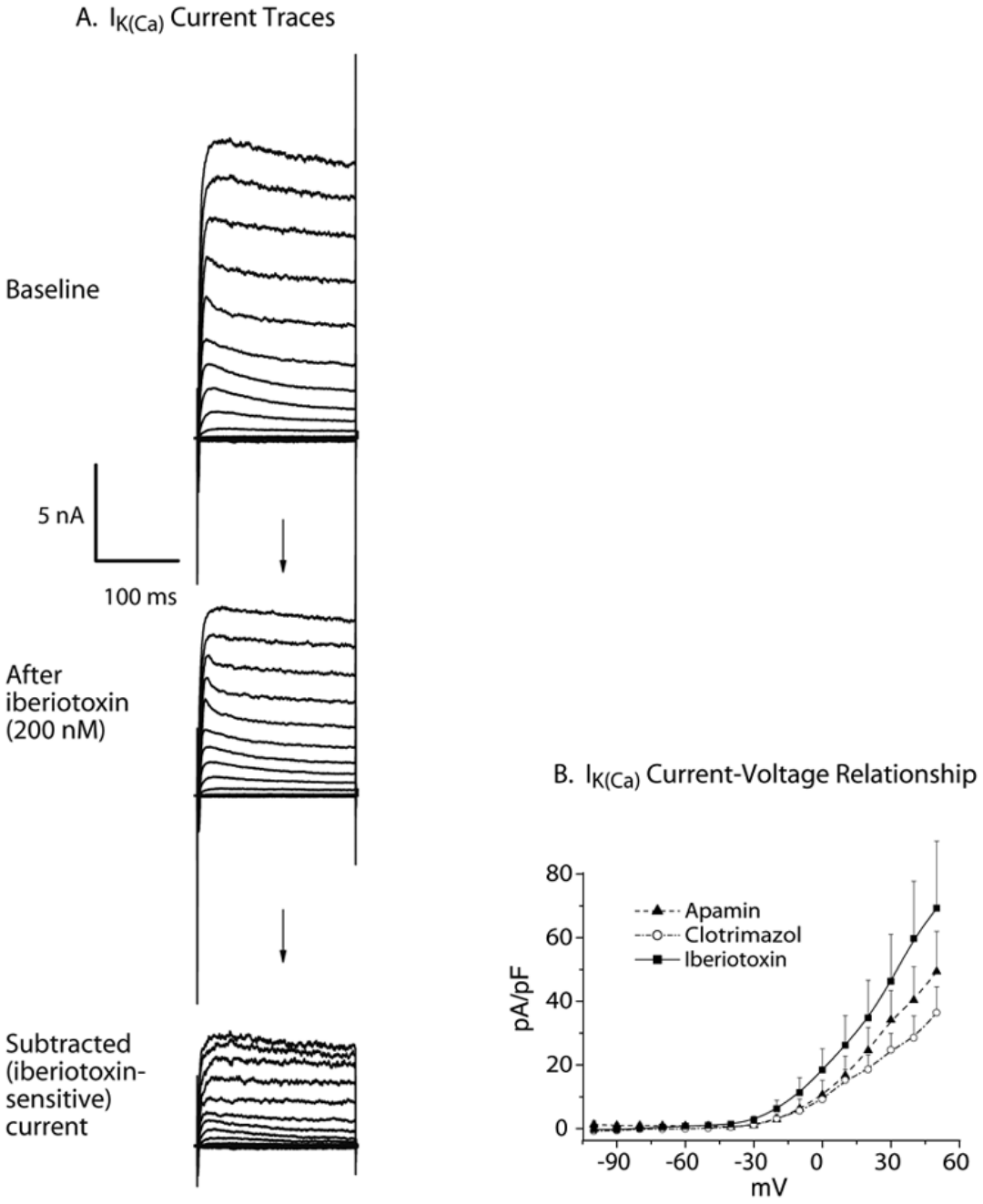

Figure 4.

A. Current traces showing response to iberiotoxin (200 nM) in an individual medium-sized control neuron. Currents were elicited from HP −60mV, with 200ms square voltage command pulses, delivered every 10s from −100 to +50mV. I_{Ca} was inhibited by low external [Ca^{2+}] and cadmium, while the cytosolic free [Ca^{2+}] was clamped at 1μM. Iberiotoxin sensitive current, indicative of BK channels, was derived by subtraction of the current after the toxin from the baseline traces. B. Control medium sized DRG neuronal somata contain apamin- (n=22), iberiotoxin- (n=16) and clotrimazole (n=12)- sensitive $K_{(Ca)}$ current components. I–V curves were constructed from averaged, subtracted current traces elicited using 200 ms square voltage commands every 10s from HP −60 mV, with steps from −100 mV to +50 mV. Cytosolic

free [Ca^{2+}] was clamped at 1μM. Only one toxin (either apamin, or iberiotoxin, or clotrimazole) was applied on each individual cell, and difference currents indicating sensitivity to this particular toxin were derived by subtracting the traces after the toxin from the baseline traces.

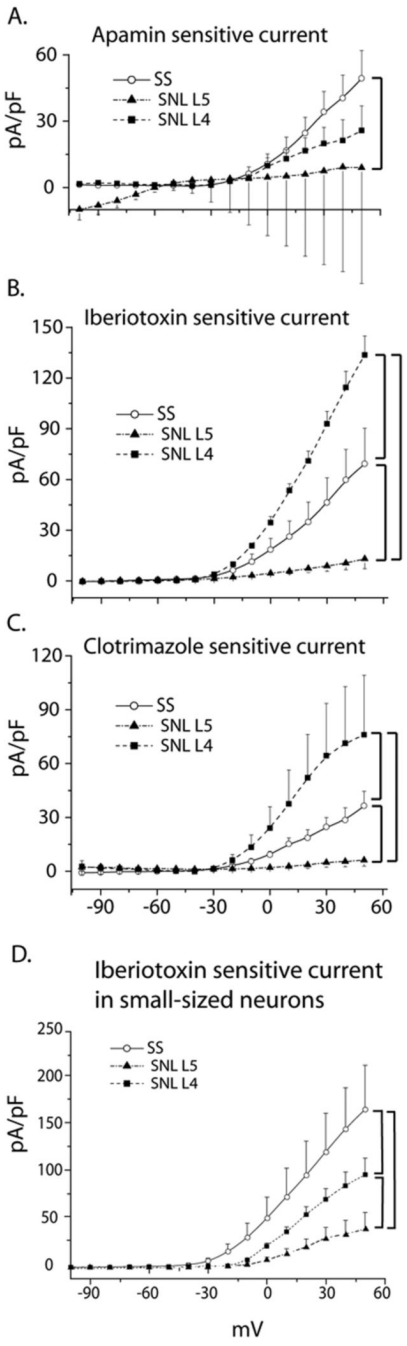

Figure 5.

Subtype-specific effects of SNL on $K_{(Ca)}$ currents in control, axotomized L5, and adjacent L4 DRG medium-sized neurons, as well as iberiotoxin-sensitive current in small-sized neurons. Figure 5A–C: I–V curves were constructed from subtracted current traces sensitive to apamin (A), iberiotoxin (B) and clotrimazole (C), elicited using 200 ms square voltage commands from HP −60 mV, after stepping from −100 mV to +50 mV. Cytosolic free $[Ca^{2+}]$ was clamped at 1μM. Bars indicate statistically significant differences between cell-types. Numbers of observations for apamin are control n=22, L5 SNL n=12, L4 SNL n=9, for iberiotoxin control n=16, L5 SNL n=9, L4 SNL n=8, and for clotrimazole control n=12, L5 SNL=9 and L4 SNL n=7. Figure 5D: Iberiotoxin-sensitive current densities indicating BK currents in control (n=6),

axotomized L5 (n=9) and adjacent L4 DRG small-sized neurons (n=12). I–V curves were constructed from subtracted current traces sensitive to 200 nM iberiotoxin elicited using 200 ms square voltage commands from HP −60 mV, after stepping from −100 mV to +50 mV. Cytosolic free [Ca^{2+}] was clamped at 1μM. Bars indicate statistically significant differences between cell-types.

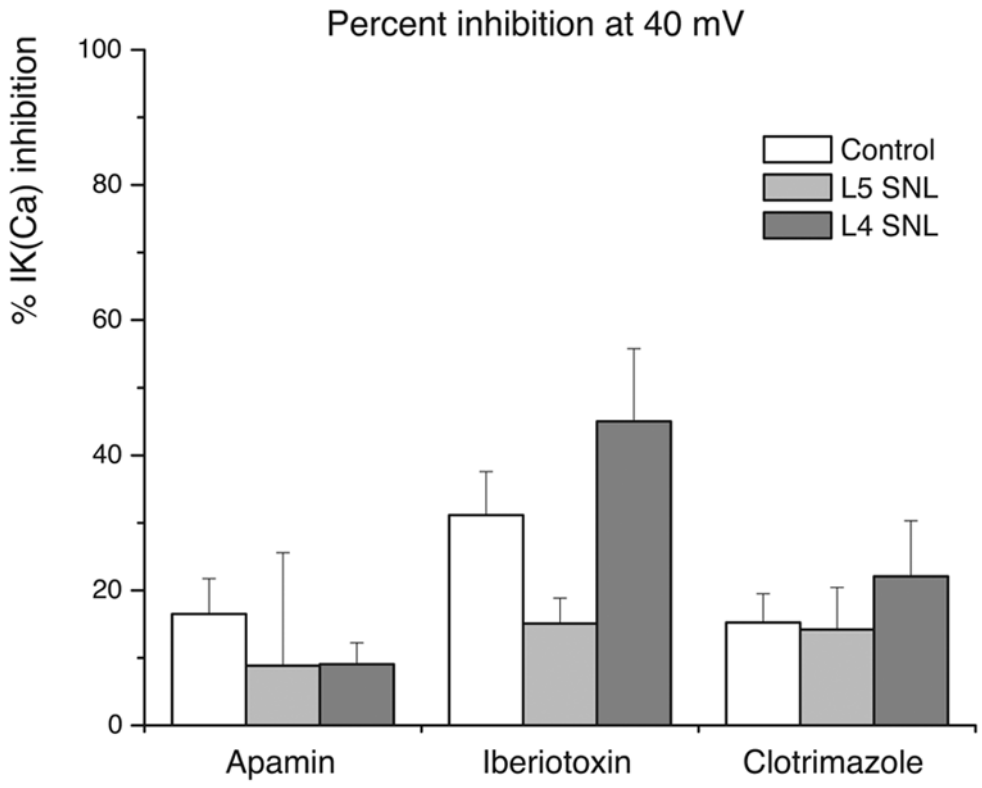

Figure 6.

Bar-graph indicating the degree of inhibition of the baseline outward current (percent inhibition from baseline), at +40 mV membrane potential, by each toxin (apamin, iberiotoxin, and clotrimazole) in control, axotomized L5 and adjacent L4 DRG medium-sized neurons. Numbers of observations are for apamin are control n=22, L5 SNL n=12, L4 SNL n=9, for iberiotoxin control n=16, L5 SNL n=9, L4 SNL n=8, and for clotrimazole control n=12, L5 SNL=9 and L4 SNL n=7.